

Chirality Selection in Open Flow Systems and in Polymerization

Yukio SAITO* and Hiroyuki HYUGA†

Department of Physics, Keio University, Yokohama 223-8522

(Received October 16, 2018)

As an attempt to understand the homochirality of organic molecules in life, a chemical reaction model is proposed where the production of chiral monomers from achiral substrate is catalyzed by the polymers of the same enantiomeric type. This system has to be open because in a closed system the enhanced production of chiral monomers by enzymes is compensated by the associated enhancement in back reaction, and the chiral symmetry is conserved. Open flow without cross inhibition is shown to lead to the chirality selection in a general model. In polymerization, the influx of substrate from the ambience and the efflux of chiral products for purposes other than the catalyst production make the system necessarily open. The chiral symmetry is found to be broken if the influx of substrate lies within a finite interval. As the efficiency of the enzyme increases, the maximum value of the enantiomeric excess approaches unity so that the chirality selection becomes complete.

KEYWORDS: homochirality, open system, polymerization, enantiomer, rate equation, dynamical chiral symmetry breaking

1. Introduction

Between two possible stereostructures of organic molecules, i.e. a right-handed (D) and a mirror-image left-handed (L) form, life on earth has chosen only one type: L-amino acids and D-sugars.¹ Various mechanisms for the origin of this chiral asymmetry, so called homochirality, have been proposed,¹ but the predicted asymmetry turned out to be very minute, and therefore, it has to be amplified to explain the homochirality.

Frank showed theoretically that an autocatalytic production of chiral molecules with an antagonistic process amplifies enantiomeric excess (ee) and brings about the homochirality.² His theory has had no experimental support for a long time. Recently, an example of ee amplification has been found in the production of pyrimidyl alkanol,³ and the temporal evolution was explained by the second-order autocatalytic reaction.⁴ In our previous papers,⁵⁻⁸ we have reported that, in addition to the nonlinear autotacalysis, recycling of achiral substrates by the decomposition of chiral products accomplishes complete homochirality in a closed system without any antagonistic processes.

The chemical reaction model we proposed⁵ involves production of a chiral molecule C from achiral molecules A and B. With an assumption that there is an ample amount of the material B, the reaction is governed solely by the concentration a of the substrate A. We adopt the convention of R, S representation to denote two enantiomers of the chiral product C as (R)-C and (S)-C, which are further abbreviated as R and S, respectively, for brevity. The reaction is assumed to include a nonlinear autocatalytic effect as well as a recycling back reaction, and the concentrations r and s of chiral species R and S develop by the following rate equations;

$$\dot{r} = (k_0 + k_1r + k_2r^2)a - \lambda_0r,$$

$$\dot{s} = (k_0 + k_1s + k_2s^2)a - \lambda_0s, \quad (1.1)$$

where \dot{x} represents the time derivative $\dot{x} = dx/dt$. The reaction system is assumed to be closed so that the concentration a of the substrate A is determined by the conservation as $a = c_0 - r - s$. Here, the constant c_0 is fixed at the initial time as $c_0 = a_0 + r_0 + s_0$. Reaction coefficients k_0 , k_1 and k_2 correspond to those in the production processes without autocatalysis, with a linear and a quadratic autocatalysis, respectively. λ_0 is a rate coefficient of decomposition process from the product R or S to the substrate A. The major conclusion we have drawn out from the model eq.(1.1) is that, only in the case with a quadratic autocatalysis and decomposition process ($k_2, \lambda > 0$), the chiral symmetry breaking is possible.⁵

However, the relevance of pyrimidyl alkanol to life is suggestive at best, and the problem of the homochirality in life is still not yet resolved. One way to address this problem is to construct a model that incorporates some characteristic features of organic molecules in life. For instance, amino acids have the potential to polymerize into chain molecules, as peptides and proteins. They act as catalysts or enzymes to produce various molecules, and among them may be amino acids themselves, although this expectation has not so far been confirmed experimentally. Based upon this hypothesis, Sandars⁹ proposed a "toy model" for the generation of homochirality such that polymers catalyze production process of chiral monomers from achiral substrates. He included cross inhibition effect such that the addition of wrong handed enantiomer to the polymer halts further polymerization.^{9,10} The cross inhibition is similar to the mutual destruction effect introduced by Frank. In this paper, we would like to propose an alternative model for the generation of homochirality, exploiting a characteristic feature that reactions take place in an open system; we do not require processes of cross inhibition.

Most of amino acids (19 out of 20 species) are chiral,

*yukio@rk.phys.keio.ac.jp

†hyuga@rk.phys.keio.ac.jp

but they are composed of achiral molecules as carbon dioxides, ammonium, water and so on. These achiral substrates are supplied from and leave away to the ambience. On the other hand, the products, amino acids, polymerize to form peptides and proteins, which not only function as catalysts or enzymes but also are used for many other purposes as body construction, metabolism, etc. This means that some amino acids leak away from the reaction path of catalysts production: The chiral products thus flow out from the reaction system in concern. All these features lead us to the necessity to study an open system. We construct a minimal reaction model including the above ingredients. In a certain limit, we can show that open reaction systems are reducible to our previous model eq.(1.1) or similar models in a closed system.⁵

In the following section §2, a simple model of chiral molecule production under an open flow is shown to behave similar to that in a closed system after a transient time. In §3, the polymerization model is studied, and the open flow is found necessary to break the chiral symmetry for this model. The results are summarized in the last section §4. Some details of stability analysis is relegated in the appendix.

2. Chemical Reaction in an Open System under Flow

First we extend our nonlinear autocatalytic system proposed previously⁵ to an open system under flow, and show that a flow plays essentially the same role as the recycling process in a closed system.

As for the origins of the incoming flow, substrate molecules A may be produced by some chemical reactions inside the system, or there may be a supply of A's by a flow from ambience. In any case, the incoming flux of A is assumed to be constant and is denoted as F . On the other hand, dissipation may be due to the outgoing flow which takes away part of all the chemical species from the region where the reactions are taking place. For simplicity the rate of outflow is assumed common to all chemical species, and denoted as μ_0 . Combining the effects of autocatalytic chemical reaction and in- and out-flows, the rate equations are written as

$$\begin{aligned}\dot{r} &= f(r)a - \lambda_0 r - \mu_0 r, \\ \dot{s} &= f(s)a - \lambda_0 s - \mu_0 s, \\ \dot{a} &= -(f(r) + f(s))a + \lambda_0(r + s) + F - \mu_0 a.\end{aligned}\quad (2.1)$$

Here $f(r) = k_0 + k_1 r + k_2 r^2$ is the production rate of R including the effect of autocatalysis, $f(s)$ is the corresponding one for S, λ_0 is the rate of back reaction from chiral products R or S to the substrate A. It is then easy to show that the sum of all the species relax to a constant value $c_0 = F/\mu_0$ in a relaxation time μ_0^{-1} as $r + s + a = c_0 + (r_0 + s_0 + a_0 - c_0) \exp(-\mu_0 t)$. Thus, after the relaxation time μ_0^{-1} , the open system we consider reduces effectively to a closed system (1.1) at a fixed total concentration c_0 with a modified back reaction rate $\lambda = \lambda_0 + \mu_0$. The difference between the two systems is essentially the value of c_0 ; in a closed system it is determined as an initial condition, whereas in an open system

it is controlled by the in- and out-going flows. Therefore, even in the case that the back reaction is absent ($\lambda_0 = 0$), the outflow plays essentially the same role as the back reaction, and the chirality selection can be realized in combination with nonlinear autocatalysis. This conclusion leads us to propose an experiment of the Soai reaction³ under the flow with an expectation that the complete homochirality can be realized.

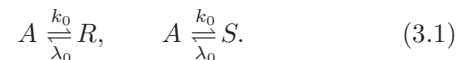
The analysis in this section reveals that the generic form of the model (1.1) has a wide range of applicability to describe the chirality selection in various systems. In the following section in the analysis of polymerization processes, we encounter a generalized form of this type of rate equations

$$\begin{aligned}\dot{r} &= f(r)a - \lambda(r)r \\ \dot{s} &= f(s)a - \lambda(s)s,\end{aligned}\quad (2.2)$$

where $f(r)$ is an effective production rate and $\lambda(r)$ is an effective rate of back reaction. The substrate concentration a follows another generic equation. Equation (2.2) does not contain the cross inhibition term such as $-\lambda_c r s$. By suitable conditions for the functions $f(r)$, $\lambda(r)$ and other parameters, the chirality selection is realized as is demonstrated in the following. Some of the details is described in the Appendix.

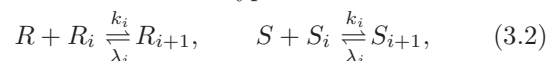
3. Chirality Selection in Polymerization

We now study the chiral symmetry breaking in the catalyst polymerization processes. Our model starts from chemical reactions of chiral molecule production from achiral substrate, as

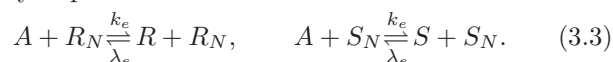


Here an achiral substrate A reacts to produce chiral species R and S with a rate k_0 and the reverse reaction takes place with a rate λ_0 . R and S symbolize two enantiomeric forms of amino acids in L and D forms. We call them R and S chiral monomers respectively hereafter. Since the production of amino acids requires energy, the rate k_0 is very small. Only in some special environment and places, for instance under thunderstorms or close to seafloor hydrothermal vent, the energy is supplied to increase k_0 . But if there is only the enhancement of random production by k_0 , then the racemic mixture of R and S monomers results, as is shown in the following. Thus, for chirality selection, we have to consider further mechanism.

Chiral monomers are assumed to polymerize if they are of the same enantiomeric type as



with $i = 1, 2, \dots$. Here k_i and λ_i represent respectively the polymerization and decomposition rate of the chiral polymers R_{i+1} or S_{i+1} . Generally, polymers at higher levels or macromolecules have some chemical functions. When the N -mers, R_N and S_N , act as enzymes to reproduce the monomer of the same enantiomeric type, the catalytic process is described as



Here k_e represents the rate of catalytic production and λ_e that of back reaction. A good enzyme should have a large production rate k_e compared to k_0 , that of the non-autocatalytic production process. However, the ratio of rate coefficients of a forward and a backward reactions is specified by the energy difference of initial and final states, A and R (or S). Then the back reaction with λ_e should also be enhanced so as to satisfy the following relation

$$\frac{\lambda_e}{k_e} = \frac{\lambda_0}{k_0}. \quad (3.4)$$

For simplicity, further polymerization starting upward from the enzyme N -mers will not be considered in the following; namely, the reaction processes (3.2) only up to $i \leq N - 1$ are considered here.

While the whole system is described by the reaction processes (3.1-3.3) for a closed system, there are other processes for an open system; that is the exchange of substrate molecules between the system and the environment E as is illustrated as



and the leakage of polymers out of this system into the environment as



The leakage process does not necessarily mean the outflow of the materials to the ambience but can be consumptions of polymers for other utilities.

In the present paper, we consider the simplest case such that the dimer is sufficient to present catalytic effect, and assume $N = 2$. Then, the concentrations of achiral substrate a and of chiral products up to the dimers r , r_2 , s , s_2 evolve respectively as

$$\begin{aligned} \dot{r} &= k_0 a - \lambda_0 r + k_e a r_2 - \lambda_e r_2 r - 2k_1 r^2 + 2\lambda_1 r_2 - \mu_1 r, \\ \dot{r}_2 &= k_1 r^2 - \lambda_1 r_2 - \mu_2 r_2, \\ \dot{s} &= k_0 a - \lambda_0 s + k_e a s_2 - \lambda_e s_2 s - 2k_1 s^2 + 2\lambda_1 s_2 - \mu_1 s, \\ \dot{s}_2 &= k_1 s^2 - \lambda_1 s_2 - \mu_2 s_2 \\ \dot{a} &= -2k_0 a + \lambda_0 (r + s) - k_e a (r_2 + s_2) + \lambda_e (r_2 r + s_2 s) \\ &\quad + F - \mu_0 a. \end{aligned} \quad (3.7)$$

These rate equations yield that the total concentration of molecules $c = a + r + 2r_2 + s + 2s_2$ evolves according to

$$\dot{c} = F - \mu_0 a - \mu_1 (r + s) - 2\mu_2 (r_2 + s_2). \quad (3.8)$$

Let us first consider a closed system with $F = \mu_i = 0$, ($0 \leq i \leq 2$). Then c remains constant $c = c_0$. Even with this conservation law, rate equations are still too complicated to study the chirality selection analytically, since there are many variables coupled nonlinearly. Therefore, we utilize a steady-state approximation⁸ such that the dimerization proceeds promptly and one may set $\dot{r}_2 = \dot{s}_2 = 0$. Then the steady-state concentrations of dimers are determined in terms of monomers as

$r_2 = (k_1/\lambda_1)r^2$ and $s_2 = (k_1/\lambda_1)s^2$, and the rate equations for the monomers reduce to

$$\begin{aligned} \dot{r} &= (k_0 + \frac{k_e k_1}{\lambda_1} r^2) (a - \frac{\lambda_0}{k_0} r) \\ \dot{s} &= (k_0 + \frac{k_e k_1}{\lambda_1} s^2) (a - \frac{\lambda_0}{k_0} s) \end{aligned} \quad (3.9)$$

with $a = c_0 - (r + s) - 2(r_2 + s_2)$. Here the relation eq.(3.4) is used. Dimer enzymes lead to nonlinear autocatalytic effect, but the effect is compensated by the same amount of enhanced back reaction. Since $k_0 + (k_e k_1/\lambda_1)r^2$ and $k_0 + (k_e k_1/\lambda_1)s^2$ are always positive, the sole possible fixed point is racemic: $\bar{r} = \bar{s} = (k_0/\lambda_0)\bar{a}$. Only in the absence of the back reaction, $\lambda_0 = \lambda_e = 0$, the system has a fixed line $a = 0$. There is no chirality selection if the system has a fixed line, as was pointed out in the previous studies of a closed system.^{5,6}

From the above analysis, it is concluded that the polymerization system (our model at least) has to be open for the chiral symmetry breaking to occur. To analyse the open system theoretically, we again use the steady-state approximation by replacing the dimer concentrations by their stationary values, $r_2 = k_1 r^2 / (\lambda_1 + \mu_2)$, $s_2 = k_1 s^2 / (\lambda_1 + \mu_2)$. The approximation does not alter the structure of the fixed points for the system. The reduced rate equations for monomers are obtained as

$$\begin{aligned} \dot{r} &= (k_0 + \frac{k_e k_1}{\lambda_1 + \mu_2} r^2) a \\ &\quad - (\lambda_0 + \frac{\lambda_e k_1}{\lambda_1 + \mu_2} r^2 + \mu_1 + \frac{2\mu_2 k_1}{\lambda_1 + \mu_2} r) r, \\ \dot{s} &= (k_0 + \frac{k_e k_1}{\lambda_1 + \mu_2} s^2) a \\ &\quad - (\lambda_0 + \frac{\lambda_e k_1}{\lambda_1 + \mu_2} s^2 + \mu_1 + \frac{2\mu_2 k_1}{\lambda_1 + \mu_2} s) s. \end{aligned} \quad (3.10)$$

The enantiomeric excess order parameter of the monomer is defined by

$$\phi_1 = \frac{r - s}{r + s}. \quad (3.11)$$

From eq.(3.10) it is shown to evolve according to

$$\dot{\phi}_1 = A\phi_1 - B\phi_1^3 \quad (3.12)$$

with

$$\begin{aligned} A &= B - \frac{2k_0 a}{r + s}, \\ B &= \frac{k_1 (r + s)}{2(\lambda_1 + \mu_2)} [ak_e - \lambda_e (r + s) - 2\mu_2]. \end{aligned} \quad (3.13)$$

One notices that λ_0 , μ_0 and μ_1 do not appear explicitly in eq.(3.13), but their effects are implicitly included in the values of concentrations, a and $r + s$.

As long as the concentrations a and $r + s$ are positive, the coefficient B is always larger than A . If A is positive asymptotically or at a fixed point, then ϕ_1 approaches to a nonzero value as $\phi_1^2 = A/B$ and the chiral state will be selected. For example, if $A > 0$ at racemic fixed points ($\bar{r} = \bar{s}$), they are unstable and the system may evolve to chiral fixed points. On the contrary, if $A < 0$ at racemic fixed points, they are stable. For $\mu_0 = \mu_2 = 0$,

the racemic fixed point is easily obtained from eq.(3.7) and eq.(3.8) as

$$\bar{r} = \bar{s} = \frac{F}{2\mu_1}, \quad \bar{a} = \frac{\mu_1 + \lambda_0 + (\lambda_e k_1 / \lambda_1) \bar{r}^2}{k_0 + (k_e k_1 / \lambda_1) \bar{r}^2} \bar{r}. \quad (3.14)$$

By using the relation eq.(3.4), the coefficient A in eq.(3.13) is written as

$$A = -k_e \times \frac{\lambda_e (k_1 \bar{r}^2 / \lambda_1)^2 - (\mu_1 - 2\lambda_0) (k_1 \bar{r}^2 / \lambda_1) + \lambda_0 (\lambda_0 + \mu_1) / \lambda_e}{k_e (k_1 \bar{r}^2 / \lambda_1) + k_0}. \quad (3.15)$$

Therefore, A is positive and the racemic fixed point is unstable, if the influx F is in the range between the lower bound F_1 and the upper one F_2 , given as

$$F_{1,2} = \mu_1 \sqrt{\frac{2\lambda_1}{\lambda_e k_1} \left(\mu_1 - 2\lambda_0 \mp \mu_1 \sqrt{1 - 8\lambda_0 / \mu_1} \right)} \quad (3.16)$$

with $\mu_1 > 8\lambda_0$. This region where the racemic fixed point is unstable is denoted by "chiral" in the $F - \lambda_0/k_0$ phase space in Fig.1(a). Parameters are fixed at $k_0 = 0.1$, $k_1 = 1$, $k_e = 10$ as well as at $\lambda_1 = \mu_1 = 1$, and the decomposition rates back to achiral substrate λ_0, λ_e are varied by keeping the relation (3.4) satisfied. At a very large F , the racemic fixed point recovers stability, since $\bar{r} = \bar{s}$ increase and the chirality suppression factor $\lambda_e(\bar{r} + \bar{s})$ in B due to a finite back reaction rates $\lambda_{0,e}$ exceeds the chirality enhancement factor $\bar{a}k_e \approx \lambda_e \bar{r}$. Therefore, by decreasing the back reaction, the racemic fixed point is expected to remain unstable at large F . Actually, at $\lambda_0 = \lambda_e = 0$, the upper bound F_2 diverges and the instability of racemic fixed point takes place for all F 's larger than the lower bound

$$F_1 = 2\mu_1 \sqrt{\frac{\lambda_1 k_0}{k_1 k_e}}. \quad (3.17)$$

When the back reaction is too strong as $\lambda_0 > \mu_1/8$, or when the substrate influx is too strong as $F \gg F_2$, there remain plenty of achiral substrates and the random production by k_0 dominates over the catalytic production with k_e . When the substrate influx is too weak as $F < F_1$, there are too few product chiral molecules to sustain catalytic chiral enhancement. In those regions, racemic fixed point is the only possibility. With a small decomposition $\lambda_0 < \mu_1/8$ and with a moderate substrate influx, states with broken chirality are possible.

We note that the conclusions of the instability on the racemic fixed point remain valid for the full system, irrespective of the approximations. Equipped with these results, we carry out numerical integration of the full rate equations (3.7) systematically. All concentrations except r (or s) are set zero initially, and the initial value of r (or s) is varied to obtain the flow trajectories. The flow diagram in the phase space of the total concentrations of two enantiomers, $r_\Sigma = r + 2r_2$ and $s_\Sigma = s + 2s_2$, shows that the chiral symmetry breaking actually takes place in the region denoted by "chiral" in Fig.1(a). For example, flow trajectories at $F = 0.5$ with $\lambda_0/k_0 = \lambda_e/k_e = 0.6$ in Fig.2(a) clearly shows the symmetry breaking: Fixed points with broken chiral symmetry attract all the trajectories.

The degree of chiral symmetry breaking is measured by the total enantiomeric excess

$$\phi = \frac{r_\Sigma - s_\Sigma}{r_\Sigma + s_\Sigma}. \quad (3.18)$$

Within the chiral region, the fixed point value of ϕ varies as the incoming flux F , as shown in Fig.3(a). Due to the symmetry, there is a trivial symmetric branch with negative ϕ values, which is not shown. Near above the lower bound F_1 , the ee increases continuously. Here, chiral fixed points lie close to the racemic one, and the parameter A in eq.(3.13) is approximately written as $A \propto (F - F_1)(F_2 - F)$. Since the F and \bar{r} are small, contributions of dimers r_2 in r_Σ is negligibly small. Thus $\phi \approx \phi_1 \propto \sqrt{F - F_1}$.

As F increases, ϕ increases as well, and the chiral fixed point extends for F larger than F_2 , where the racemic fixed point recovers its stability. In fact, for F between F_2 and F_3 there are two types of stable fixed points, racemic and chiral, in the flow diagram, as shown in Fig.2(b) at $F = 0.8$. If the initial concentrations r and s for the numerical integration of eq.(3.7) are close to the racemic configuration, the final state remains racemic, since it is stable, at least locally, as proven by the stability analysis. However, if the integration start from a well developed chiral configuration, the chiral fixed point is selected. The concentration phase space of r 's and s 's is thus divided into multiple basins of attractions to racemic and chiral fixed points. When F is larger than F_3 , the basins of attraction to the chiral fixed points seem to disappear.

From Fig.2(b) it is evident that for F between F_2 and F_3 there are unstable chiral fixed points (marked by white diamonds) between the racemic and stable chiral fixed points (marked by black boxes). Therefore, in the $F - \phi$ diagram in Fig.3(a), there is another branch corresponding to these unstable chiral fixed points, denoted by a dashed curve: it extends from F_3 back to the small F direction below the stable chiral branch. The unstable branch seems to be connected to the F axis at a point F_2 .

The maximum value of ee in Fig. 3 is rather small. This is due to the present choice of a parameter set, especially k_0 , which is chosen rather large on purpose so that the fixed points are clearly discernible in figures. With a parameter set in Fig.2(a), for example, the ee takes a value $\phi = 0.871$, but with a smaller value of k_0 as $k_0 = 0.01$, the ee increases up to $\phi = 0.992$ and the stable chiral fixed points lie almost on two axes.

Every aspect of the phase boundary and the flow trajectories remains the same, even if all the out-flow rates μ_i take finite values, for example $\mu_0 = \mu_1 = \mu_2 = 1$: Phase diagram in F versus λ_0/k_0 in Fig.1(b) looks similar to that in Fig.1(a). When F takes the value between F_1 and F_2 , the racemic fixed point is unstable and the chiral symmetry breaks as shown in Fig.2(c). Between F_2 and F_3 , there is a hysteresis such that the stationary state depends on the initial concentrations of r 's and s 's. From the lower bound F_1 the ee increases continuously until it drops suddenly to zero at F_3 , as shown in Fig.3(b), where the expected unstable chiral fixed points are omitted.

We now consider cases without any direct back reaction, $\lambda_i = 0$ for $i = 1$ to 3. Still, part of chiral products is utilized for other purposes and disappears from the catalyst production route, such that μ_i 's are finite. By fixing $\mu_0 = \mu_2 = 1$ and at various μ_1 , the chiral symmetry breaking is achieved at an incoming flux F larger than the lower bound, as shown in Fig.4(a). One notices that there is a minimum in the lower bound of the incoming flux F . With $\mu_0 = \mu_1 = \mu_2 = 1$, the ee increases rapidly to the saturation value ϕ close to unity, as shown in Fig.3(c). With small k_0 and large k_e , the saturation to $\phi = 1$ happens almost instantaneously.

With finite rates of back reactions, as $\lambda_i = k_i$ for example, the out-going μ_1 has to be sufficiently large to realize the chirality selection, as shown in Fig.4(b). The symmetry breaking is possible for F between F_1 and F_3 with hysteresis above F_2 , similar to the previous cases in Fig.1(a) and (b). The ee increases continuously from zero at the lower bound F_1 , and drops abruptly to vanish at the upper bound F_3 with hysteresis above F_2 , as shown in Fig.3(d).

4. Summary and Discussions

We extend our model of chiral molecule production from achiral substrate with nonlinear autocatalysis to an open system under flow. Even if the back reaction is not explicitly included, the system after a transient period is shown to be effectively described by the rate equations we derived for a closed system with back reaction, and the chirality selection is expected to take place. As an ideal system to realize homochirality in laboratory, we proposed the Soai reaction under flow.

Organic molecules in life, amino acids for instance, may not undergo nonlinear autocatalytic reaction, but they polymerize and acquire some functions. One of them is to catalyze various chemical reactions, presumably the monomer production process as well. We construct a model of chiral monomer production from achiral substrate with further polymerization to produce enzymes which enhance monomer production of the same enantiomeric type. By assuming for simplicity that dimers already act as enzymes, the rate equations of monomer concentrations reduce to those with quadratic autocatalysis in a steady-state approximation. In a closed system, however, the enzyme enhances the decomposition process as well, and the chiral symmetry is not broken. Only in an open system where substrate is supplied and parts of produced monomers and polymers are consumed for other purposes, the chiral symmetry can be broken if parameters take proper values. Influx of substrate should be large to yield sufficient chiral products to sustain catalytic process, but if the back reaction takes place the influx should not be too large. Otherwise, an enhanced back reaction compensates the chirality enhancement.

We have considered only a single chiral species for simplicity reason, whereas in reality there are 20 types of amino acids. If only the same enantiomeric type can form stable polymers, we believe that the present mechanism of chirality selection is still valid for multiple chiral species.

By extending the ladder for polymerization processes

until the enzyme is produced, the window in parameter space for the chiral symmetry breaking becomes narrower. Various disturbances due to spatial and temporal variations may tend to narrow this window further. However narrow the parameter window may be, it is essential that the window is open. After all, it seems to be a majority consensus that several hundred million years were needed for the birth of life on the earth.

Acknowledgement

Authors acknowledge support from the Gakuji-Shinkou-Shikin by Keio University.

Appendix

A general set of the (reduced) rate equations for the concentrations r, s, a is

$$\begin{aligned}\dot{r} &= f(r)a - \lambda(r)r \\ \dot{s} &= f(s)a - \lambda(s)s \\ \dot{c} &= g(a) - h(r) - h(s) \\ c &= a + j(r) + j(s)\end{aligned}\tag{A.1}$$

where $f(r)$ and $\lambda(r)$ are the effective coefficients of the production reaction and the back reaction, respectively. c is the total concentration and functional forms of $g(a), h(r), j(r)$ depend on models but presumably are nonnegative functions. An enantiomeric excess order parameter defined as

$$\phi = \frac{r - s}{r + s}\tag{A.2}$$

is shown from eq. (A.1) to evolve according to

$$\dot{\phi} = A\phi - B\phi^3\tag{A.3}$$

with

$$\begin{aligned}A &= B - \frac{2f(0)a}{r + s} \\ B &= \frac{1}{2}(r + s) \\ &\times \left\{ \frac{s(f(r) - f(0)) - r(f(s) - f(0))}{rs(r - s)}a - \frac{\lambda(r) - \lambda(s)}{r - s} \right\}\end{aligned}\tag{A.4}$$

The form of the parameter B is so chosen that it remains finite for the racemic state $r = s$ as well as at the trivial point $r = s = 0$. For specific form $f(r) = k_0 + k_1r + k_2r^2$ and $\lambda(r) = \lambda_0 + \lambda_1r + \lambda_2r^2$, B becomes simply

$$B = \frac{1}{2}(r + s)\{k_2a - \lambda_1 - \lambda_2(r + s)\}.\tag{A.5}$$

We should not forget that A and B are functions of the variable r, s, a and varies as functions of time accordingly.

For simplicity, let us assume that $\bar{r}\bar{s}\bar{a} \neq 0$ at a fixed point $r = \bar{r}$, $s = \bar{s}$, $a = \bar{a}$, which satisfy

$$f(\bar{r})\bar{a} = \lambda(\bar{r})\bar{r}, \quad f(\bar{s})\bar{a} = \lambda(\bar{s})\bar{s}.\tag{A.6}$$

Using these equations, one obtains

$$\bar{B} = \frac{1}{2}(\bar{r} + \bar{s})\frac{f(0)\bar{a}}{\bar{r}\bar{s}}\tag{A.7}$$

and $\bar{A} = \bar{\phi}^2\bar{B}$. The last relation only shows the consistency. To analyse the stability of the fixed point, one

should first to obtain the fixed point values of a, r, s as functions of relevant parameters and finds the conditions for the chiral phase $A > 0$ or for the racemic phase $A \leq 0$ as is discussed in section 3.

The other way to analyse the stability is the linear stability analysis. As a concrete example, we consider the stability matrix for the full system eq.(3.7) at the racemic fixed point eq.(3.14) supplemented with $\bar{r}_2 = k_1 \bar{r}^2 / (\lambda_1 + \mu_2)$, $\bar{s}_2 = k_1 \bar{s}^2 / (\lambda_1 + \mu_2)$. Since there are five independent variables as $(x_1, x_2, x_3, x_4, x_5) \equiv (r, r_2, s, s_2, a)$, the linear deviation around a fixed point \bar{x}_i is assumed to be $x_i = \bar{x}_i + x_{i0} \exp(\Omega t)$. The equation to determine the eigenfrequency Ω is an eigenvalue equation $|\Gamma - \Omega I| = 0$, where I is the 5×5 dimensional unit matrix and the matrix elements of Γ are given as $\Gamma_{ij} = \partial \dot{x}_i / \partial x_j$ evaluated at the fixed point. In a matrix form, it is expressed as

det

$$\begin{pmatrix} -S - \Omega & T & 0 & 0 & U \\ 2k_1 \bar{r} & -\lambda_1 - \Omega & 0 & 0 & 0 \\ 0 & 0 & -S - \Omega & T & U \\ 0 & 0 & 2k_1 \bar{r} & -\lambda_1 - \Omega & 0 \\ V & W & V & W & -2T - \Omega \end{pmatrix} = 0 \quad (\text{A}\cdot 8)$$

where the nonzero matrix elements are given as

$$\begin{aligned} S &= \mu_1 + \lambda_0 + 4k_1 \bar{r} + \lambda_e \bar{r}_2 \\ T &= 2\lambda_1 + k_e \bar{a} - \lambda_e \bar{r} \\ U &= k_0 + k_e \bar{r}_2 \\ V &= \lambda_0 + \lambda_e \bar{r}_2 \end{aligned} \quad (\text{A}\cdot 9)$$

$$W = -k_e \bar{a} + \lambda_e \bar{r}.$$

This equation is expressed as a product of a quadratic and a cubic equations as

$$\begin{aligned} & [\Omega^2 + (S + \lambda_1)\Omega + S\lambda_1 - 2k_1 T \bar{r}] \\ & \times [-(\Omega + S)(\Omega + \lambda_1)(\Omega + 2U) \\ & + 2k_1 T \bar{r}(\Omega + 2U) + 2UV(\Omega + \lambda_1) + 4UWk_1 \bar{r}] = 0. \end{aligned} \quad (\text{A}\cdot 10)$$

The instability condition for the racemic fixed point is the existence of positive eigenfrequency. As $S + \lambda_1 > 0$ is always satisfied, an inequality $S\lambda_1 - 2k_1 T \bar{r} < 0$ is just the condition for the quadratic equation to have a positive root and it can be shown that this condition agrees with that given in section 3. As for the cubic equation, its roots are near $-S < 0$, $-\lambda_1 < 0$, $-2T < 0$ and thus are expected to be negative. Numerically we confirmed this expectation for reasonable parameter ranges.

- 1) B. L. Feringa and R. A. van Delden: *Angew. Chem. Int. Ed.* **38** (1999) 3418.
- 2) F. C. Frank: *Biochim. Biophys. Acta* **11** (1953) 459.
- 3) K. Soai, T. Shibata, H. Morioka and K. Choji: *Nature* **378** (1995) 767.
- 4) I. Sato, D. Omiya, H. Igarashi, K. Kato, Y. Ogi, K. Tsukiyama and K. Soai: *Tetrahedron Asymmetry* **14** (2003) 975.
- 5) Y. Saito and H. Hyuga: *J. Phys. Soc. Jpn* **73** (2004) 33.
- 6) Y. Saito and H. Hyuga: *J. Phys. Soc. Jpn* **73** (2004) 1685.
- 7) Y. Saito and H. Hyuga: *Progr. Chem. Phys. Res.* (2005) to appear.
- 8) Y. Saito and H. Hyuga: *J. Phys. Soc. Jpn.* **74** (2005) No.2.
- 9) P.G.H. Sandars, *Orig. Life Evolu. Biosph.* **33** (2003) 575.
- 10) A. Brandenburg, A.C. Andersen, S. Hoefner and M. Nilsson, *Orig. Life Evol. Biosph.* (2004) to appear.

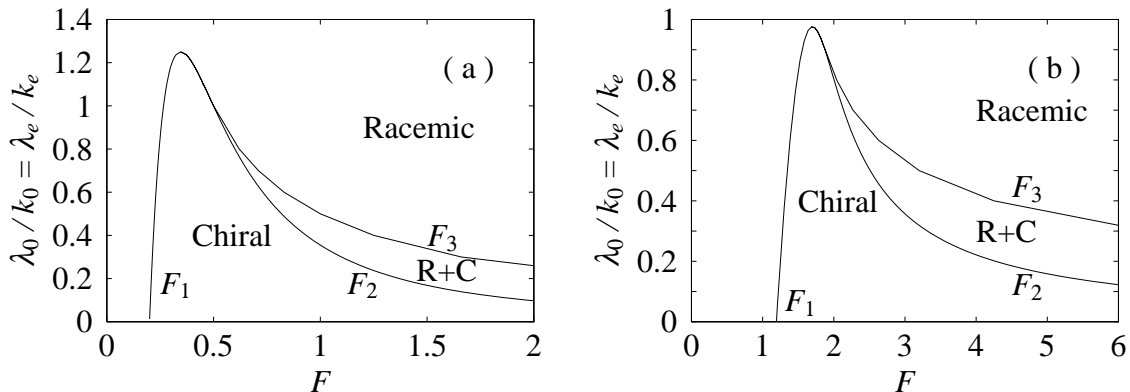


Fig. 1. Phase boundary between the racemic and the chiral fixed points in the $F - \lambda_0/k_0$ phase space. Production parameters are fixed at $k_0 = 0.1$, $k_1 = 1$, $k_e = 10$. Other parameters fixed are (a) $\mu_0 = \mu_2 = 0$, $\lambda_1 = \mu_1 = 1$, and (b) $\mu_{0,1,2} = \lambda_1 = 1$.

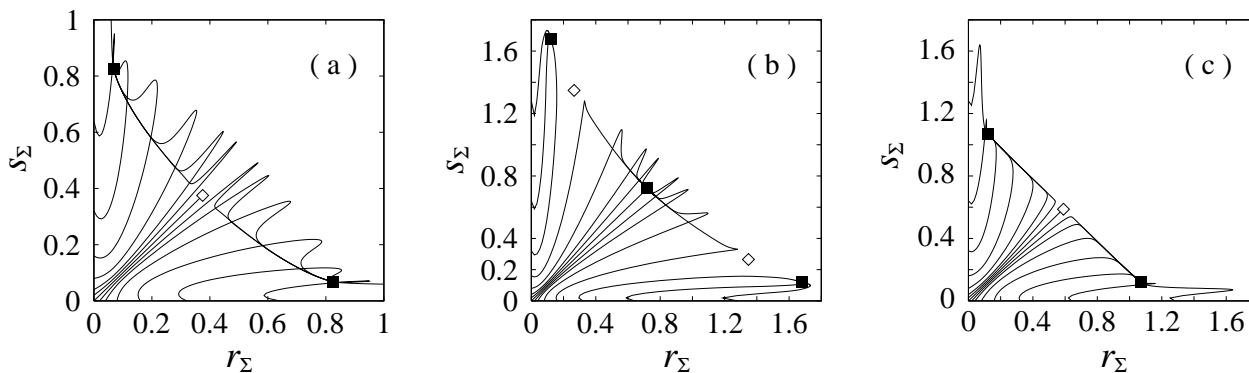


Fig. 2. Flow diagram in the total concentrations of r and s phase space. Black boxes represent stable fixed points, and white diamonds unstable ones. Production parameters are fixed at $k_0 = 0.1$, $k_1 = 1$, $k_e = 10$. Figures (a) and (b) correspond to Fig.1(a) with decomposition rates $\lambda_1 = 1$, $\lambda_0/k_0 = \lambda_e/k_e = 0.6$ and flow $\mu_0 = \mu_2 = 0$. The in-coming flux of the substrate is (a) $F = 0.5$ and (b) $F = 0.8$. (c) corresponds to Fig.1(b) with decomposition rates $\lambda_1 = 1$, $\lambda_0/k_0 = \lambda_e/k_e = 0.5$ and flow $\mu_0 = \mu_1 = \mu_2 = 1$. The in-coming flux of the substrate is $F = 2$.

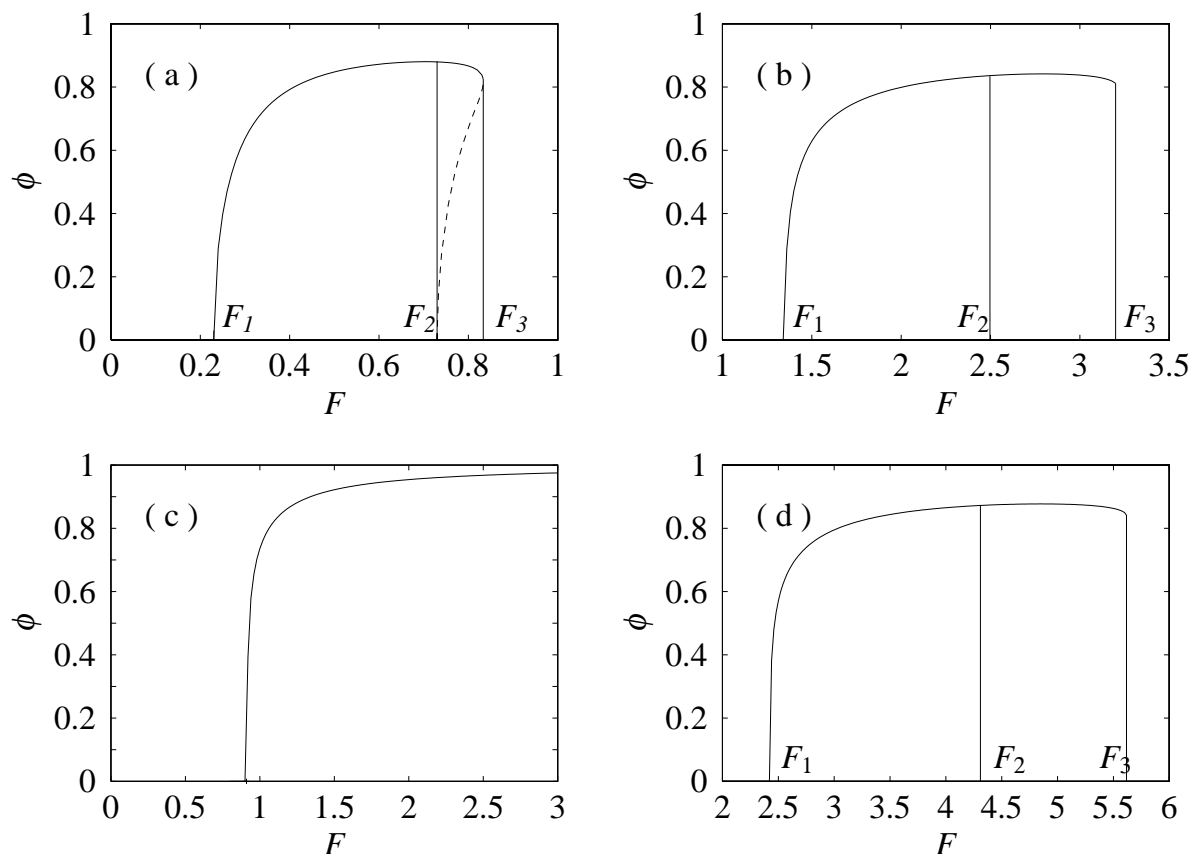


Fig. 3. Fixed point value of the total enantiomeric excess ϕ versus influx F . Production parameters are fixed at $k_0 = 0.1$, $k_1 = 1$, $k_e = 10$. Figure (a) corresponds to Fig.1(a) with decomposition rates $\lambda_1 = 1$, $\lambda_0/k_0 = \lambda_e/k_e = 0.6$ and out-flow $\mu_1 = 1$, $\mu_0 = \mu_2 = 0$. (b) corresponds to Fig.1(b) with decomposition rates $\lambda_1 = 1$, $\lambda_0/k_0 = \lambda_e/k_e = 0.5$ and out-flow $\mu_0 = \mu_1 = \mu_2 = 1$. (c) corresponds to Fig.4(a) without decompositions, $\lambda_i = 0$ and out-flow $\mu_0 = \mu_1 = \mu_2 = 1$. (d) corresponds to Fig.4(b) with decompositions $\lambda_i = k_i$ and out-flow $\mu_0 = \mu_2 = 1$, $\mu_1 = 2$.

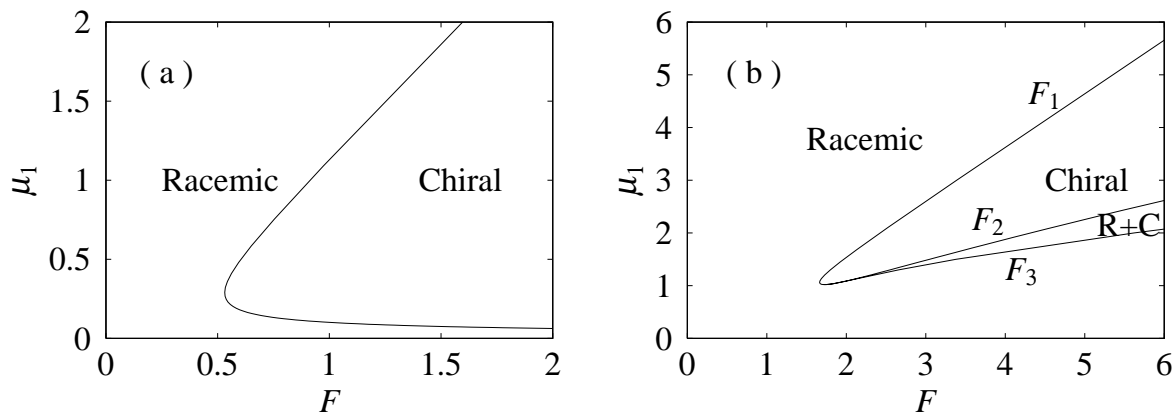


Fig. 4. Phase boundary between the racemic and the chiral fixed points in the $F - \mu_1$ phase space. Production parameters are fixed at $k_0 = 0.1$, $k_1 = 1$, $k_e = 10$, and $\mu_0 = \mu_2 = 1$. Rates of back reactions are (a) $\lambda_i = 0$, and (b) $\lambda_i/k_i = 1$ with $i = 0, 1, e$.